Research article

Weichun Huang*, Chunyang Ma, Chao Li, Ye Zhang, Lanping Hu, Tingting Chen, Yanfeng Tang, Jianfeng Ju and Han Zhang*

Highly stable MXene (V_2CT_x)-based harmonic pulse generation

https://doi.org/10.1515/nanoph-2020-0134
Received February 20, 2020; accepted May 3, 2020

Abstract: MXene as a novel two-dimensional (2D) material exhibits a lot of advantages in nonlinear optics. However, the common MXene, $Ti_3C_2T_x$ and Ti_2CT_x nanosheets, easily suffer from degradation under ambient conditions, greatly limiting their practical applications. Here, we demonstrated one of MXene compounds, V_2CT_x, which has a strong modulation depth (nearly 50%), can serve as an excellent saturable absorber (SA) in passively mode-locked (PML) fiber lasers. More importantly, 206th harmonic order has been successfully generated in Er-doped mode-locked fiber laser, exhibiting maximum repetition rate of 1.01 GHz and pulse duration of 940 fs, which to the best of our knowledge, is the highest harmonic mode-locked fiber laser from the MXene SA so far. In addition, the high harmonic order mode-locked operation can maintain at least 24 h without any noticeable change, suggesting MXene V_2CT_x nanosheets have excellent stability in this mode-locked fiber laser. It is anticipated that the present work can pave the way to new design for MXene-based heterostructures for high-performance harmonic mode-locked lasers.

Keywords: harmonic pulse generation; layered materials; mode-locked fiber lasers; MXene; V_2CT_x.

1 Introduction

Passively mode-locked (PML) fiber lasers have been attracted great attention due to their low-cost, simplification, high beam quality, *etc*. As we know, saturable absorber (SA) plays an important role in PML fiber lasers, which can be divided into two categories, *i. e*., real SAs and artificial SAs. Artificial SAs, such as nonlinear polarization evolution (NPE) and nonlinear optical loop mirror (NOLM), can easily achieve ultrashort pulses from laser cavity [1–4]. However, NPE is unstable under ambient environment, and NOLM needs precise control in the powering splitting. Semiconductor SA mirror is the most general real SAs applied in ultrafast lasers [5, 6], but the slow saturation recovery and narrow operation bandwidth limit its applications.

Recently, two dimensional (2D) materials are of great interest due to their special electronic structure and excellent physical and chemical properties [7–10], especially as a SA in the field of ultrafast lasers. Although graphene has been successfully inserted into the PML laser system [11-15], yet the zero band gap energy and low modulation depth greatly limits its wide applications. Topological insulators and transition metal dichalcogenides have also been investigated as potential SA in ultrafast lasers while their poor photoresponse behaviours make them limited in the broadband photoresponse mode-locked laser system [16–22]. Black phosphorus has also been employed as a potential SA in ultrafast lasers [23–28], but the environmentally unstable property results into the fast degradation under ambient conditions, making them

***Corresponding authors: Weichun Huang**, Nantong Key Lab of Intelligent and New Energy Materials, School of Chemistry and Chemical Engineering, Nantong University, Nantong, 226019, Jiangsu, PR China; Collaborative Innovation Center for Optoelectronic Science & Technology, International Collaborative Laboratory of 2D Materials for Optoelectronics Science and Technology of Ministry of Education, Institute of Microscale Optoelectronics, Shenzhen University, Shenzhen, 518060, PR China, E-mail: huangweichun@ntu.edu.cn; and **Han Zhang**, Collaborative Innovation Center for Optoelectronic Science & Technology, International Collaborative Laboratory of 2D Materials for Optoelectronics Science and Technology of Ministry of Education, Institute of Microscale Optoelectronics, Shenzhen University, Shenzhen, 518060, PR China, hzhang@szu.edu.cn. https://orcid.org/0000-0002-1948-8347 (W. Huang), https://orcid.org/0000-0002-9131-9767 (H. Zhang)
Chunyang Ma, Chao Li and Ye Zhang: Collaborative Innovation Center for Optoelectronic Science & Technology, International Collaborative Laboratory of 2D Materials for Optoelectronics Science and Technology of Ministry of Education, Institute of Microscale Optoelectronics, Shenzhen University, Shenzhen, 518060, PR China
Lanping Hu, Tingting Chen, Yanfeng Tang and Jianfeng Ju: Nantong Key Lab of Intelligent and New Energy Materials, School of Chemistry and Chemical Engineering, Nantong University, Nantong, 226019, Jiangsu, PR China

severely unsatisfied in the practical applications. In addition, it should be noted that rapid growing attention has been focused on MXene materials due to their remarkable optoelectronic and optical properties and has been applied into various applications [29–33]. The general formula of MXene is $M_{n+1}X_nT_x$, where M is an early transition metal, X is C and/or N, T is the surface terminations (hydroxyl, oxygen or fluorine), and n = 1, 2, or 3, respectively [34]. To date, MXenes have been successfully applied as a SA to the ultrafast laser systems. Jhon *et al.* demonstrated a stable Er-doped fiber laser based on MXene Ti_3CN with 660 fs pulse duration at the repetition rate of 15.4 MHz [35]. Jiang *et al.* reported that MXene $Ti_3C_2T_x$ was employed as a SA for mode-locking operation at 1066 and 1555 nm, respectively, and a high stable femtosecond laser with pulse duration as short as 159 fs in the telecommunication window was readily obtained [34]. Li *et al.* delivered a highly stable femtosecond fiber laser based on MXene $Ti_3C_2T_x$ with signal-to-noise (SNR) ratio up to 70.7 dB and central wavelength of 1567.3 nm [36]. Wu *et al.* reported that an all-optical device based on an MXene Ti_2CT_x-deposited microfiber knot resonator exhibited a large photothermal conversion efficiency and high thermal conductivity, showing that the proposed all-optical device was capable of producing a high-performance phase and intensity modulation with a high modulation efficiency, fast response time, and good stability [37]. Although the common MXene ($Ti_3C_2T_x$ or Ti_2CT_x) presented outstanding performance as a SA in ultrafast pulse, yet they easily suffered from oxidation under ambient conditions, leading to the formation of primarily anatase (TiO_2), which is still of critical importance to their application [38, 39].

In all-anomalous regime, pulses can be easily split into multi-pulses due to exceed nonlinear phase shift with the increase of pump power, even at which it is harmful for achieving high energy pulses, while it is still suitable for harmonic pulse generation. Compared with the fundamental state, harmonic mode-locking state can achieve higher repetition rate pulses. High repetition rate pulse can be widely used in the fields of fiber sensing [40], optical communications [41], frequency comb [42], *etc.* So far, there are rare reports on the harmonic mode-locking fiber laser based on MXene. Very recently, harmonic mode-locking based on MXene SA has been demonstrated, but the repetition rate is only 218.4 MHz with 36th harmonic mode-locking [43]. Therefore, it is crucial to develop the high-performance harmonic mode-locked fiber laser based on MXene SA, including the high repetition rate and excellent stability.

In this work, MXene V_2CT_x nanosheets were synthesized by selective etching of Al element from V_2AlC, similar to the reported $Ti_3C_2T_x$ [44, 45] and Ti_2CT_x [46, 47], and deposited onto a ring fiber cavity as a SA to achieve 206th high order harmonic mode-locking for the first time. The nonlinear saturated absorption of this 2D layered MXene V_2CT_x has been systematically investigated, demonstrating that the modulation depth and saturation intensity are nearly 50% and 0.5 mW, respectively, which suggests that V_2CT_x can serve as a potential SA in ultrafast lasers. By increasing the pump power, 206th harmonic mode-locking can be easily generated with the central wavelength and 3 dB bandwidth are 1559.1 nm with 3.1 nm, respectively, and the repetition rate can reach up to 1.01 GHz with 940 fs pulse duration, in this work. Moreover, the high harmonic order mode-locked operation can maintain at least 24 h without any noticeable change, suggesting MXene V_2CT_x nanosheets have excellent stability in this mode-locked fiber lasers.

2 Experimental section

2.1 Materials

V_2AlC powder (99.9%), isopropyl alcohol (IPA, 99.9%), hydrofluoric acid (HF) (40%) were purchased from Sigma–Aldrich. Double distilled deionized (DI) water was used for the synthesis.

2.2 Synthesis of MXene V_2CT_x nanosheets

The MXene V_2CT_x nanosheets were synthesized by selective etching of Al element from V_2AlC. For example, 2.0 g V_2AlC (200 mesh) was added into 40 mL hydrofluoric acid (HF) (40%) under continuous stirring at 30 °C for 48 h. After the reaction, the mixture was diluted by a large amount of DI H_2O, and then centrifugated for a couple of times (5,000 rpm, 10 min per cycle) until the pH of the supernatant was more than 6. The V_2C was obtained by filtration through a polyvinylidene fluoride membrane (0.45 μm mesh) and washed with a large quantity of DI H_2O (~2 L). The as-obtained V_2C slurry was first dispersed into DI H_2O (~5 mg mL^{-1}), followed by a sonication process in a water bath with a built-in water-cooling system for 8 h at 400 W. The temperature was fixed at 10 °C in the whole sonication process. Afterwards, the dispersion was initially centrifuged at a speed of 5,000 rpm for 30 min, and then the supernatant containing V_2CT_x nanosheets was gently decanted to another test tube and further centrifuged at a centrifugation speed of 18,000 rpm for another 30 min. The obtained precipitate was dried at 80 °C in vacuum.

2.3 Characterization

The morphologies and dimensions of V_2C and V_2CT_x nanosheets were determined by both SEM (Hitachi-SU8010) and transmission electron microscope (TEM) (FEI Tecnai G2 F30). High-resolution TEM (HRTEM) was performed to determine the atomic arrangements of the as-obtained V_2CT_x nanosheets. The height of the as-synthesized MXene V_2CT_x nanosheets was evaluated by atomic force microscopy (AFM, Bruker, with 512 pixels per line) measurement with an AFM sample prepared by dropping the MXene V_2CT_x nanosheets dispersion onto a clean silicon substrate. UV–Vis–NIR absorption spectra were collected with spectral range of 200–1100 nm by a UV–Vis–NIR absorbance spectrometer (Cary 60, Agilent) at room temperature.

3 Results and discussion

Figure 1 gives structural characterization of the as-etched V_2C and as-exfoliated V_2CT_x nanosheets. The basal planes fan out and spread apart after HF treatment (Figure 1a), confirming the successful removal of Al from V_2AlC. The TEM image of the exfoliated nanosheets (Figure 1b) indicates that the as-exfoliated V_2CT_x nanosheets are quite thin due to much higher transparency in comparison with super-thin carbon film. The lateral size of V_2CT_x nanosheets ranges from ~130 to ~240 nm. The crystal structure of the as-prepared V_2CT_x nanosheets can be further confirmed by HRTEM and selected area electron diffraction (SAED), shown in Figure 1c, in good agreement with previous demonstrations [48]. The AFM was employed to determine the thickness of the as-prepared V_2CT_x nanosheets, as shown in Figure 1d. The few-layer V_2CT_x nanosheets with thicknesses of 9.8 and 11.2 nm, respectively, were successfully obtained (insert in Figure 1d), corresponding to around 11 layers of MXene V_2C [49, 50]. Figure 1e shows the absorption spectrum of the V_2CT_x nanosheets, ranging from 250 nm to 1800 nm, implying the broad bandwidth operation of this material. Notably, the absorption spectrum of the MXene V_2CT_x nanosheets remains unchanged after MXene V_2CT_x nanosheets/IPA stored for 10 days, suggesting their excellent stability under ambient conditions, which was also evidenced by after-ten-day TEM measurement (Figure S1).

The adsorption process of the material was observed in real time by a microscope. Figure S2 shows the experiment

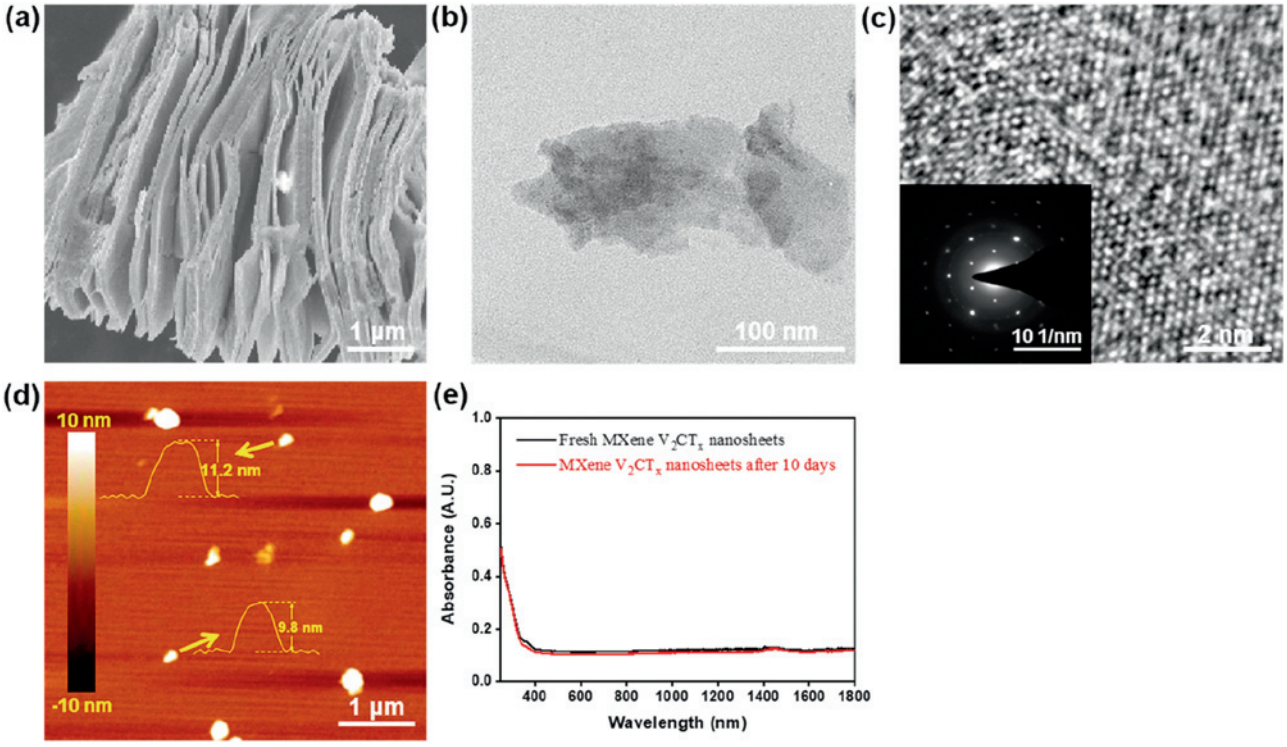

Figure 1: Structural characterization of as-synthesized V_2CT_x nanosheets. (a) SEM image of V_2C after selective removal of Al. (b) TEM image of exfoliated V_2CT_x nanosheets. (c) HRTEM of exfoliated V_2CT_x nanosheets. (d) AFM image of exfoliated V_2CT_x nanosheets. (e) UV–Vis–NIR spectroscopy of exfoliated V_2CT_x nanosheets before and after 10 days.

of MXene V_2CT_x nanosheets deposition on a tapered fiber. The nonlinear absorption measurement of the MXene-based SA was carried out using a balanced twin-detector (Figure 2a). An ultrashort pulsed fiber laser (800 fs pulse duration, 1558 nm wavelength and 45.9 MHz pulse repetition frequency) was used as the pump light source. The output was split by a 50:50 fiber coupler after an adjustable attenuator, and one beam was used for detecting the nonlinear absorption of SA while the other for power monitoring as a reference signal. By continuous adjustment of the attenuator, the transmitted power as a function of the incident optical power was recorded for the V_2CT_x-SA device. The transmission of the SA tends to be a constant with the increase of the peak power intensity. The transmission is a nonlinear curve indicative of saturable absorption which has the standard model:

$$T(I) = 1 - \frac{\alpha_s}{1 + I/I_{sat}} - \alpha_{ns}$$

where α_s is the modulation depth, I is the power of the input light, I_{sat} is the saturable power, and α_{ns} is the non-saturated loss. The fitting results in Figure 2b can be expressed as $T(I) = 0.788 - 0.488/(1 + I/0.2)$. The modulation depth and the saturation power of the MXene are estimated to 48.8% and 0.5 mW, respectively (Figure 2b). The strong saturable-absorption property of the V_2CT_x-SA at 1558 nm indicates that this device can be used as an ultrafast optical switch for ultrashort pulse generation.

The experimental set up of the Er-doped PML fiber laser based on V_2CT_x-SA is shown in Figure 3. A laser diode with the central wavelength of 976 nm serves as a pump. The light couples into the cavity via a 980/1550 wavelength division multiplexer (WDM). Polarization controller enables a thorough and continuous adjustment of the net cavity birefringence and the isolator ensures unidirectional propagation. A fiber optical coupler (OC) split ratio is 10:90, which allows 10% power energy as output. MXene SA is spliced into cavity *via* tapered fiber and the nonlinear

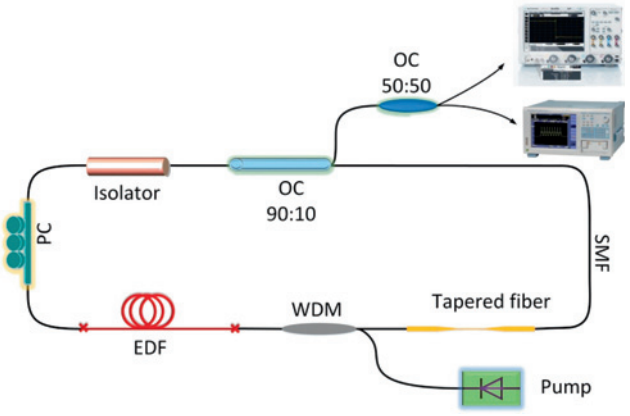

Figure 3: Experimental setup of the PML fiber lasers based on MXene V_2CT_x nanosheets as SA. EDF: Erbium-doped fiber, PC: polarization controller.

effects can be enhanced by reducing the effective mode area in tapered fiber, which greatly accelerates the formation of the harmonic mode-locked operation. The total cavity length is ~31 m, and the total dispersion is –0.6 ps^2. The PML fiber lasers based on MXene V_2CT_x nanosheets was systematically measured by a suit of equipment, consisting of an optical spectrum analyzer (Yokogawa AQ6370D), an autocorrelator (APE pulseCheck), an oscilloscope (Keysight DSOS104 A) and a radio-frequency (RF) analyzer (Keysight N9010B) with a high-speed photodetector.

The laser cavity reached mode-locked operation at a threshold pump power of 27 mW. Figure 4 shows the output performance from the Er-doped PML fiber laser. The output spectrum at 3 dB is 0.9 nm at the central wavelength of 1559.12 nm (Figure 4a). Figure 4b shows the pulse train within the span of 1000 ns and the pulse interval is around 201 ns. The figure inserted in the screen was captured from the oscilloscope (time range is 10 μs), which reflects that pulse train is ultra-stable in the laser cavity, indicating the

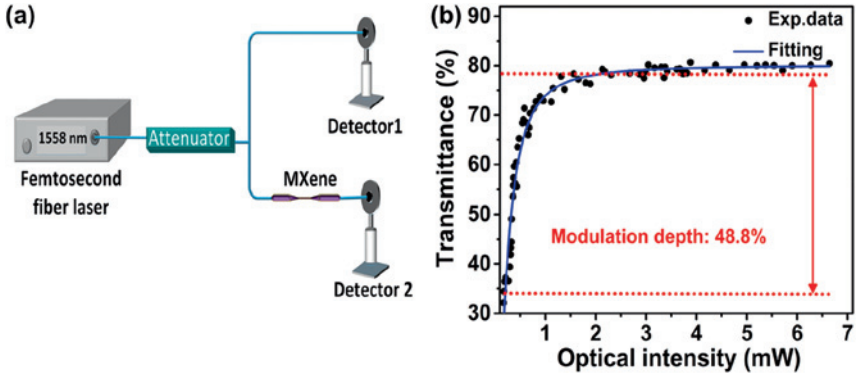

Figure 2: Nonlinear optical measurement of V_2CT_x. (a) Nonlinear transmittance detector system. (b) Nonlinear transmission of V_2CT_x nanosheets at 1558 nm.

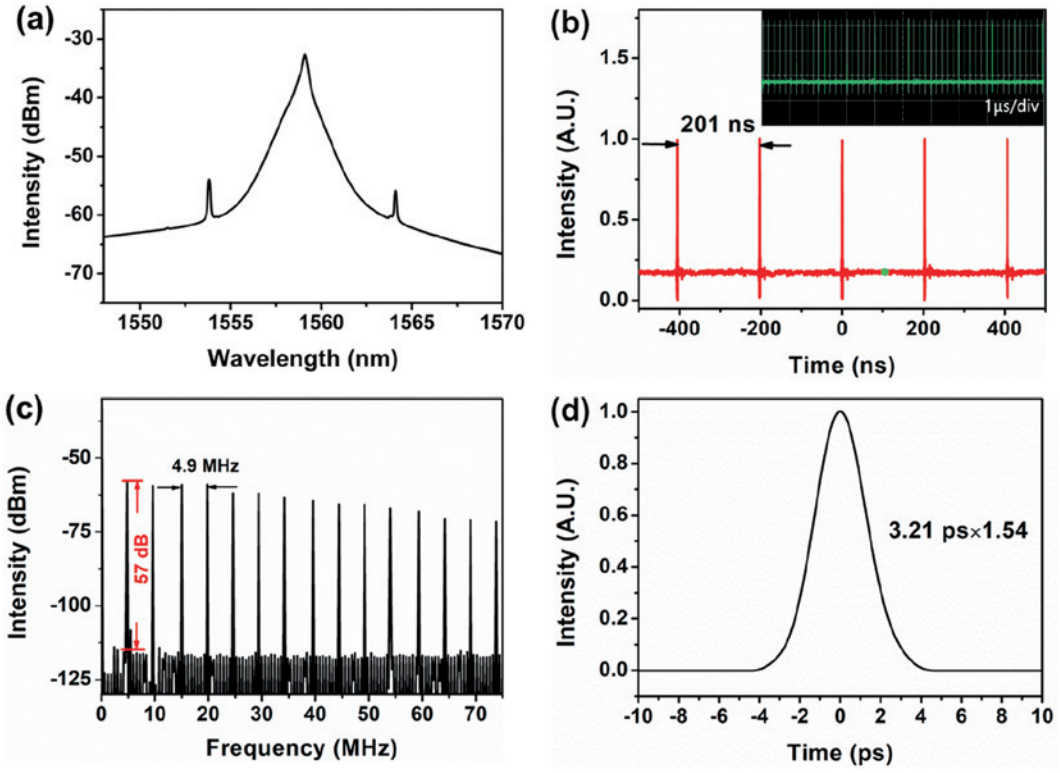

Figure 4: Fundamental mode-locked operation. (a) Optical spectrum. (b) Corresponding pulse train. (c) RF spectrum. (d) Autocorrelation.

great potential application in the field of the Er-doped PML fiber laser. RF spectrum of the signal exhibits that the SNR is approximately 57 dB and the fundamental repetition is 4.9 MHz (Figure 4c), further suggesting the stability of the laser system. In addition, the pulse duration was measured by the autocorrelation instrument and fitted by the function of hyperbolic secant, and the pulse duration is 3.21 ps. The time bandwidth product is around 0.351, indicating that the output pulse has a weak chirp.

In all-anomalous regimes, pulse can be easily split into multi-pulse because the laser cavity cannot endure the nonlinear phase shift with the increase of the pump power. Hence, harmonic mode-locked operation can be easily achieved by increasing the pump power. The harmonic pulse train of different orders (121st, 167th and 206th) with the span of 20 ns can be obtained, as shown in Figure 5a–c and Figure S2. The maximum harmonic pulse of 206th has been successfully achieved when the pump power increases to 540 mW. The pulse train is within 10 ns and the pulse interval is approximately 1.001 ns (Figure 5c). The inserted figure (screen captured from oscillator) shows the pulse train within 1 μs, from which it can be clearly observed that the pulse train is ultra-stable, indicating its easy control in the practical applications. Figure 5d shows the spectrum with central wavelength of 1559.1 nm and 3 dB bandwidth of 3.1 nm. It can be observed in Figure 5e that the signal peak and the SNR in RF spectrum are 1.01 GHz and 55 dB, respectively. The autocorrelation of the harmonic pulses demonstrates that the pulse duration is 940 fs fitted by the function of hyperbolic secant and the time bandwidth product is around 0.359 (Figure 5f), indicating that the output still has weak chirp.

Figure 6a shows that the harmonic order and output power *versus* pump power. It can be seen that the repetition rate increases from 4.9 MHz to 1.01 GHz with the increase of pump power (27–580 mW). The high input power confirms that V_2CT_x-SA has a high damage threshold, combined with an excellent nonlinear effect of V_2CT_x, and the maximum harmonic order can reach 206th at a pump power of 580 mW, which is the highest achieved harmonic mode-locked fiber laser from an MXene SA. Notably, the V_2CT_x-SA in this work also presents the overall high performances, compared with the reported 2D materials (Table 1), due to the MXene unique properties. In addition, the high harmonic order mode-locked operation can maintain for at least 24 h without any noticeable changes, indicating an ultra-stable mode-locked laser system based on V_2CT_x SA (Figure 6b). Combined with the high modulation depth (nearly 50%) of V_2CT_x, it proved that V_2CT_x can be an ideal candidate SA for PML fiber lasers, which can provide fundamental guidance

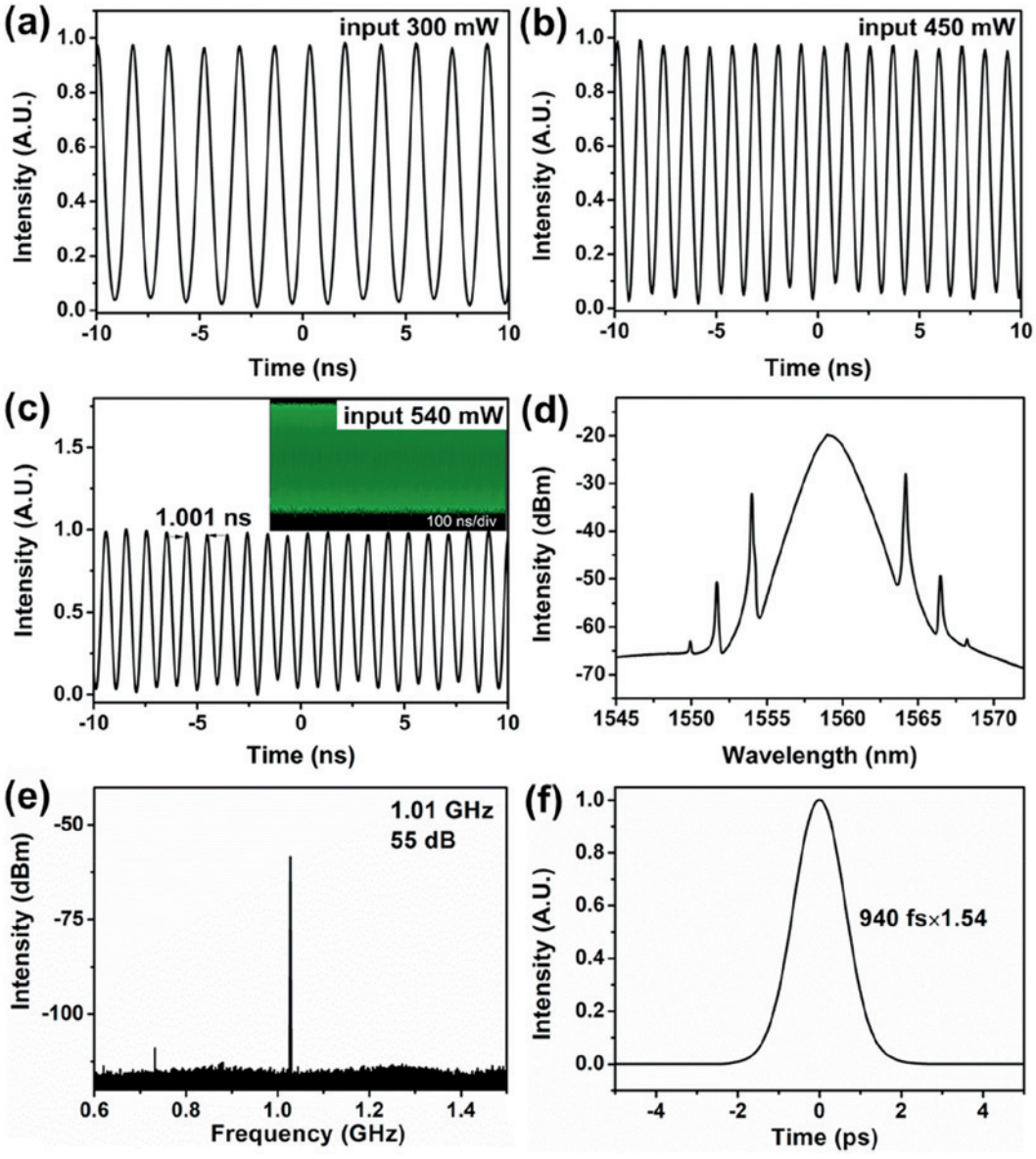

Figure 5: Harmonic mode-locked operation based on MXene V_2CT_x nanosheets. (a) Pulse train at pump power of 300 mW. (b) Pulse train at pump power of 450 mW. (c) Pulse train at pump power of 540 mW. (d) Optical spectrum. (e) RF spectrum. (f) Autocorrealtion.

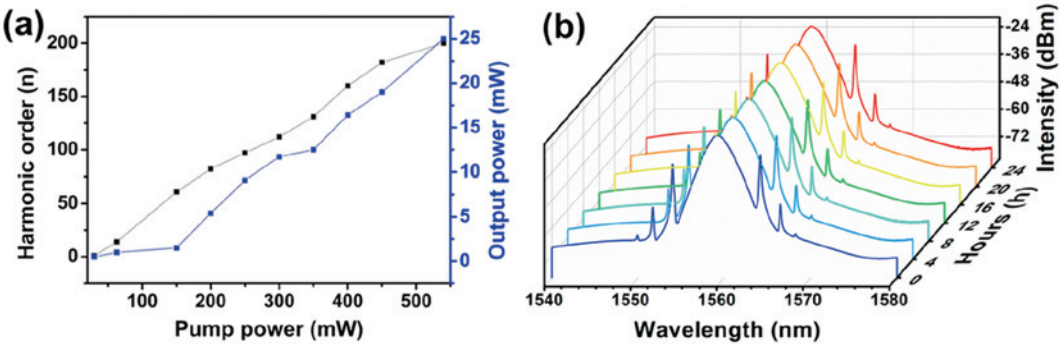

Figure 6: Output performance based on V_2CT_x. (a) Harmonic order and output power versus pump power. (b) Spectrum by increasing hours.

Table 1: Comparison of output performance of 1.5 μm harmonic mode-locked fiber lasers based on 2D materials.

	Modulation depth (%)	Repetition rate (GHZ)	Pulse duration (ps)	Harmonic order	SNR (dB)	Ref.
Graphene	–	0.56	10.45	101	–	[51]
$SnSe_2$	6.38	0.26	0.887	31	12	[40]
WS_2	11	0.46	0.66	45	66	[52]
Bi_2Te_3	3.75	0.77	0.63	55	63	[53]
Sb_2Te_3	–	0.30	2.2	81	55	[54]
$Ti_3C_2T_x$	0.96	0.22	0.85	36	36	[43]
V_2CT_x	48.8	1.01	0.94	206	55	This work

on the new design of MXene $V_2CT_{x\text{-based}}$ heterostructures for high-performance mode-locked fiber lasers.

4 Conclusion

In summary, MXene V_2CT_x nanosheets were successfully synthesized by selective etching method and directly deposited onto the microfiber to facilitate light–matter interaction between V_2CT_x nanosheets and the evanescent field of microfiber. It was demonstrated that the Er-doped passively mode-locked fiber laser based on V_2CT_x SA exhibited the 206th order harmonic mode-locked (1.01 GHz repetition rate) with 940 fs pulse duration with the increase of the pump power, which, to the best of our knowledge, is the highest harmonic mode-locked fiber laser from an MXene SA so far. In addition, with regard to the degradation of common MXene under ambient conditions, such as $Ti_3C_2T_x$ and Ti_2CT_x, the long-term stability measurement of MXene V_2CT_x nanosheets confirms that they have greater potential into the practical applications. Because of facile fabrication, easy harmonic pulse generation and environmental stability, it is expected that MXene V_2CT_x can shed light on new design for MXene-based heterostructures to construct high-performance mode-locked fiber lasers.

Acknowledgement: W. H. and C. M. contributed equally to this work. The research was supported by the National Natural Science Foundation of China (Grant No. 61805147, and 61875138), and the Science and Technology Innovation Commission of Shenzhen (Grant No. JCYJ20180305125141661, and KQTD2015032416270385). The authors gratefully acknowledge the Materials and Devices Testing Center at Graduate School at Shenzhen, Tsinghua University, Shenzhen 518055, P. R. China.

Author contribution: All the authors have accepted responsibility for the entire content of this submitted manuscript and approved submission.

Research funding: The research was funded by the National Natural Science Foundation of China, Science and Technology Innovation Commission of Shenzhen and Materials and Devices Testing Center at Graduate School at Shenzhen, Tsinghua University.

Employment or leadership: None declared.

Honorarium: None declared.

Conflict of interest statement: The authors declare no conflicts of interest regarding this article.

References

[1] N. Kuse, J. Jiang, C. C. Lee, et al., "All polarization-maintaining Er fiber-based optical frequency combs with nonlinear amplifying loop mirror," *Optic Express*, vol. 24, pp. 3095–3102, 2016.

[2] A. Chong, L. G. Wright, and F. W. Wise, "Ultrafast fiber lasers based on self-similar pulse evolution: a review of current progress," *Rep. Prog. Phys.*, vol. 78, Art no. 113901, 2015, https://doi.org/10.1088/0034-4885/78/11/113901.

[3] B. Oktem, C. Ülgüdür, and F. Ö. Ilday, "Soliton-similariton fibre laser," *Nat. Photon.*, vol. 4, pp. 307–311, 2010.

[4] N. H. Seong and D. Y. Kim, "Experimental observation of stable bound solitons in a figure-eight fiber laser," *Opt. Lett.*, vol. 27, pp. 1321–1323, 2002.

[5] U. Keller, "Recent developments in compact ultrafast lasers," *Nature*, vol. 424, pp. 831–838, 2003.

[6] I. D. Jung, F. X. Kärtner, N. Matuschek, et al., "Semiconductor saturable absorber mirrors supporting sub-10-fs pulses," *Appl. Phys. B*, vol. 65, pp. 137–150, 1997.

[7] J. S. Ponraj, Z. Q. Xu, S. C. Dhanabalan, et al., "Photonics and optoelectronics of two-dimensional materials beyond graphene," *Nanotechnology*, vol. 27, Art no. 462001, 2016, https://doi.org/10.1088/0957-4484/27/46/462001.

[8] K. F. Mak and J. Shan, "Photonics and optoelectronics of 2D semiconductor transition metal dichalcogenides," *Nat. Photon.*, vol. 10, pp. 216–226, 2016.

[9] K. Choi, Y. T. Lee, and S. Im, "Two-dimensional van der Waals nanosheet devices for future electronics and photonics," *Nano Today*, vol. 11, pp. 626–643, 2016.

[10] A. K. Geim, "Graphene: status and prospects," *Science*, vol. 324, pp. 1530–1534, 2009.

[11] R. I. Woodward, R. C. T. Howe, G. Hu, et al., "Few-layer MoS_2 saturable absorbers for short-pulse laser technology, pp.

current status and future perspectives," *Photon. Res.*, vol. 3, pp. A30–A42, 2015.
[12] C. Zhao, H. Zhang, X. Qi, et al., "Ultra-short pulse generation by a topological insulator based saturable absorber," *Appl. Phys. Lett.*, vol. 101, Art no. 211106, 2012, https://doi.org/10.1063/1.4767919.
[13] M. Hajlaoui, E. Papalazarou, J. Mauchain, et al., "Ultrafast surface carrier dynamics in the topological insulator Bi_2Te_3," *Nano Lett.*, vol. 12, pp. 3532–3536, 2012.
[14] T. Hasan, Z. Sun, F. Wang, et al., "Nanotube-polymer composites for ultrafast photonics," *Adv. Mater.*, vol. 21, pp. 3874–3899, 2009.
[15] Q. Bao, H. Zhang, Y. Wang, et al., "Atomic-layer graphene as a saturable absorber for ultrafast pulsed lasers," *Adv. Funct. Mater.*, vol. 19, pp. 3077–3083, 2009.
[16] J. Wang, Z. Jiang, H. Chen, et al., "Magnetron-sputtering deposited WTe_2 for an ultrafast thulium-doped fiber laser," *Opt. Lett.*, vol. 42, pp. 5010–5013, 2017.
[17] W. Liu, L. Pang, H. Han, et al., "Tungsten disulphide for ultrashort pulse generation in all-fiber lasers," *Nanoscale*, vol. 9, pp. 5806–5811, 2017.
[18] W. Liu, L. Pang, H. Han, et al., "70-fs mode-locked erbium-doped fiber laser with topological insulator," *Sci. Rep.*, vol. 6, p. 19997, 2016.
[19] J. Koo, Y. I. Jhon, J. Park, et al., "Near-infrared saturable absorption of defective bulk-structured WTe_2 for femtosecond laser mode-locking," *Adv. Funct. Mater.*, vol. 26, pp. 7454–7461, 2016.
[20] J. Boguslawski, G. Sobon, R. Zybala, and J. Sotor, "Dissipative soliton generation in Er-doped fiber laser mode-locked by Sb_2Te_3 topological insulator," *Opt. Lett.*, vol. 40, pp. 2786–2789, 2015.
[21] M. Zhang, R. C. T. Howe, R. I. Woodward, et al., "Solution processed MoS_2-PVA composite for sub-bandgap mode-locking of a wideband tunable ultrafast Er: fiber laser," *Nano Res.*, vol. 8, pp. 1522–1534, 2015.
[22] J. Sotor, G. Sobon, and K. M. Abramski, "Sub-130 fs mode-locked Er-doped fiber laser based on topological insulator," *Optic Express*, vol. 22, pp. 13244–13249, 2014.
[23] C. Ma, C. Wang, B. Gao, et al., "Recent progress in ultrafast lasers based on 2D materials as a saturable absorber," *Appl Phys Rev*, vol. 6, Art no. 041304, 2019, https://doi.org/10.1063/1.5099188.
[24] M. Zhang, Q. Wu, F. Zhang, et al., "2D Black phosphorus saturable absorbers for ultrafast photonics," *Adv. Optic. Mater.*, vol. 7, Art no. 1800224, 2019, https://doi.org/10.1002/adom.201800224.
[25] X. Jin, G. Hu, M. Zhang, et al., "102 fs pulse generation from a long-term stable, inkjet-printed black phosphorus-mode-locked fiber laser," *Optic Express*, vol. 26, pp. 12506–12513, 2018.
[26] J. Du, M. Zhang, Z. Guo, et al., "Phosphorene quantum dot saturable absorbers for ultrafast fiber lasers," *Sci. Rep.*, vol. 7, p. 42357, 2017.
[27] J. Sotor, G. Sobon, W. Macherzynski, et al., "Black phosphorus saturable absorber for ultrashort pulse generation," *Appl. Phys. Lett.*, vol. 107, Art no. 051108, 2015, https://doi.org/10.1063/1.4927673.
[28] D. Li, H. Jussila, L. Karvonen, et al., "Polarization and thickness dependent absorption properties of black phosphorus: new saturable absorber for ultrafast pulse generation," *Sci. Rep.*, vol. 5, p. 15899, 2015.
[29] Q. Yang, F. Zhang, N. Zhang, and H. Zhang, "Few-layer MXene $Ti_3C_2T_x$ (T = F, O, or OH) saturable absorber for visible bulk laser," *Opt. Mater. Express*, vol. 9, pp. 1795–1802, 2019.
[30] Y. Dong, S. Chertopalov, K. Maleski, et al., "Saturable absorption in 2D Ti_3C_2 MXene thin films for passive photonic diodes," *Adv. Mater.*, vol. 30, Art no. 1705714, 2018, https://doi.org/10.1002/adma.201705714.
[31] X. Sun, B. Zhang, B. Yan, et al., "Few-layer $Ti_3C_2T_x$ (T = O, OH, or F) saturable absorber for a femtosecond bulk laser," *Opt. Lett.*, vol. 43, pp. 3862–3865, 2018.
[32] K. Hantanasirisakul, M. Q. Zhao, P. Urbankowski, et al., "Fabrication of $Ti_3C_2T_x$ MXene transparent thin films with tunable optoelectronic properties," *Adv. Electron. Mater.*, vol. 2, Art no. 1600050, 2016, https://doi.org/10.1002/aelm.201600050.
[33] O. Mashtalir, M. R. Lukatskaya, M. Q. Zhao, et al., "Amine-assisted delamination of Nb_2C MXene for Li-ion energy storage devices," *Adv. Mater.*, vol. 27, pp. 3501–3506, 2015.
[34] X. Jiang, S. Liu, W. Liang, et al., "Broadband nonlinear photonics in few-layer MXene $Ti_3C_2T_x$ (T = F, O, or OH)," *Laser Photon. Rev.*, vol. 12, Art no. 1700229, 2018, https://doi.org/10.1002/lpor.201870013.
[35] Y. I. Jhon, J. Koo, B. Anasori, et al., "Metallic MXene saturable absorber for femtosecond mode-locked lasers," *Adv. Mater.*, vol. 29, Art no. 1702496, 2017, https://doi.org/10.1002/adma.201702496.
[36] J. Li, Z. Zhang, L. Du, et al., "Highly stable femtosecond pulse generation from a MXene $Ti_3C_2T_x$ (T = F, O, or OH) mode-locked fiber laser," *Photon. Res.*, vol. 7, pp. 260–264, 2019.
[37] Q. Wu, W. Huang, Y. Wang, et al., "All-optical control of microfiber knot resonator based on 2D Ti_2CT_x MXene," *Adv. Optic. Mater.*, vol. 8, Art no. 1900977, 2020, https://doi.org/10.1002/adom.201900977.
[38] A. Rozmysłowska, W. Wojciechowski, W. Ziemkowska, et al., "Colloidal properties and stability of 2D Ti_3C_2 and Ti_2C MXenes in water," *Int. J. Electrochem. Sci.*, vol. 13, pp. 10837–10847, 2018.
[39] C. J. Zhang, S. Pinilla, N. McEvoy, et al., "Oxidation Stability of Colloidal Two-Dimensional Titanium Carbides (MXenes)," *Chem. Mater.*, vol. 29, pp. 4848–4856, 2017.
[40] J. S. Liu, X. H. Li, Y. X. Guo, et al., "$SnSe_2$ nanosheets for subpicosecond harmonic mode-locked pulse generation," *Small*, vol. 15, Art no. 1902811, 2019, https://doi.org/10.1002/smll.201902811.
[41] B. Mikulla, L. Leng, S. Sears, et al., "Broad-band high-repetition-rate source for spectrally sliced WDM," *IEEE Photon. Technol. Lett.*, vol. 11, pp. 418–420, 1999.
[42] J. J. McFerran, "Échelle spectrograph calibration with a frequency comb based on a harmonically mode-locked fiber laser: a proposal," *Appl. Optic.*, vol. 48, pp. 2752–2759, 2009.
[43] J. Feng, X. Li, T. Feng, et al., "Harmonic mode-locked Er-doped fiber laser by evanescent field-based MXene $Ti_3C_2T_x$ (T = F, O, or OH) saturable absorber," *Ann. Phys.*, vol. 532, Art no. 1900437, 2019, https://doi.org/10.1002/andp.201900437.
[44] X. Wang, X. Shen, Y. Gao, et al., "Atomic-scale recognition of surface structure and intercalation mechanism of Ti_3C_2X," *J. Am. Chem. Soc.*, vol. 137, pp. 2715–2721, 2015.
[45] M. Naguib, M. Kurtoglu, V. Presser, et al., "Two-dimensional nanocrystals produced by exfoliation of Ti_3AlC_2," *Adv. Mater.*, vol. 23, pp. 4248–4253, 2011.
[46] F. Liu, A. Zhou, J. Chen, et al., "Preparation and methane adsorption of two-dimensional carbide Ti_2C," *Adsorption*, vol.

22, pp. 915–922, 2016, https://doi.org/10.1007/s10450-016-9795-8.
[47] X. Wang, S. Kajiyama, H. Iinuma, et al., "Pseudocapacitance of MXene nanosheets for high-power sodium-ion hybrid capacitors," *Nat. Commun.*, vol. 6, p. 6544, 2015.
[48] M. Naguib, J. Halim, J. Lu, et al., "New two-dimensional niobium and vanadium carbides as promising materials for Li-ion batteries," *J. Am. Chem. Soc.*, vol. 135, pp. 15966–15969, 2013.
[49] D. Huang, Y. Xie, D. Lu, et al., "Demonstration of a white laser with V_2C MXene-based quantum dots," *Adv. Mater.*, vol. 31, Art no. 1901117, 2019, https://doi.org/10.1002/adma.201901117.
[50] A. VahidMohammadi, M. Mojtabavi, N. M. Caffrey, et al., "Assembling 2D MXenes into highly stable pseudocapacitive electrodes with high power and energy densities," *Adv. Mater.*, vol. 31, Art no. 1806931, 2019, https://doi.org/10.1002/adma.201806931.
[51] P. F. Zhu, Z. B. Lin, Q. Y. Ning, et al., "Passive harmonic mode-locking in a fiber laser by using a microfiber-based graphene saturable absorber," *Laser Phys. Lett.*, vol. 10, Art no. 105107, 2013, https://doi.org/10.1088/1612-2011/10/10/105107.
[52] L. Li, Y. Su, Y. Wang, et al., "Femtosecond passively Er-doped mode-locked fiber laser with WS_2 solution saturable absorber," *IEEE J. Sel. Top. Quant. Electron.*, vol. 23, pp. 44–49, 2017.
[53] J. Lee, J. Koo, Y. M. Jhon, and J. H. Lee, "Femtosecond harmonic mode-locking of a fiber laser based on a bulk-structured Bi_2Te_3 topological insulator," *Optic Express*, vol. 23, pp. 6359–6369, 2015.
[54] J. Sotor, G. Sobon, W. Macherzynski, and K. M. Abramski, "Harmonically mode-locked Er-doped fiber laser based on a Sb_2Te_3 topological insulator saturable absorber," *Laser Phys. Lett.*, vol. 11, Art no. 055102, 2014.Apr.12th, 2020, https://doi.org/10.1088/1612-2011/11/5/055102.

Supplementary Material: The online version of this article offers supplementary material (https://doi.org/10.1515/nanoph-2020-0134).